HHS Public Access

Author manuscript

Nat Immunol. Author manuscript; available in PMC 2015 June 01.

Published in final edited form as:

Nat Immunol. 2014 December ; 15(12): 1162–1170. doi:10.1038/ni.3026.

A miRNA upregulated in asthma airway T cells promotes T_H2 cytokine production

Laura J. Simpson[1], **Sana Patel**[1], **Nirav R. Bhakta**[2], **David F. Choy**[3], **Hans D. Brightbill**[4], **Xin Ren**[5], **Yanli Wang**[5], **Heather H. Pua**[6], **Dirk Baumjohann**[1], **Misty M. Montoya**[1], **Marisella Panduro**[1], **Kelly A. Remedios**[1], **Xiaozhu Huang**[5], **John V. Fahy**[2], **Joseph R. Arron**[3], **Prescott G. Woodruff**[2], and **Karl M. Ansel.**[1,*]

[1]Department of Microbiology & Immunology, Sandler Asthma Basic Research Center, University of California San Francisco, San Francisco, CA 94143 USA

[2]Division of Pulmonary and Critical Care Medicine, Department of Medicine, Cardiovascular Research Institute, University of California San Francisco, San Francisco, CA 94143 USA

[3]Immunology, Tissue Growth, and Repair Biomarker Discovery, Genentech, South San Francisco, CA 94080 USA

[4]Department of Immunology, Genentech, South San Francisco, CA 94080 USA

[5]Lung Biology Center, Department of Medicine, University of California San Francisco, San Francisco, CA 94143 USA

[6]Department of Pathology, Sandler Asthma Basic Research Center, University of California San Francisco, San Francisco, CA 94143 USA

Abstract

MicroRNAs (miRNAs) exert powerful effects on immune function by tuning networks of target genes that orchestrate cell behavior. We sought to uncover miRNAs and miRNA-regulated pathways that control the T_H2 responses that drive pathogenic inflammation in asthma. Profiling miRNA expression in human airway-infiltrating T cells revealed miR-19a elevation in asthma. Modulating miR-19 activity altered T_H2 cytokine production in both human and mouse T cells, and T_H2 cell responses were markedly impaired in cells lacking the entire miR-17∼92 cluster. miR-19 promotes T_H2 cytokine production and amplifies PI(3)K, JAK-STAT, and NF-κB signaling by direct targeting of PTEN, SOCS1, and A20. Thus, miR-19a up regulation in asthma may be an indicator and a cause of increased T_H2 cytokine production in the airways.

*Send correspondence to mark.ansel@ucsf.edu.

Author contribution statement: L.J.S. designed, performed, and analyzed most experiments. S.P, D.F.C. H.D.B., X.R., Y.W., H.H.P, D.B., M.M.M., M.P., and K.A.R. helped design and perform some experiments. X.H. helped design animal airway allergy experiments. N.R.B. analyzed human miRNA expression data. P.G.W., J.V.F., and J.R.A. designed and helped perform the clinical study for human miRNA expression analysis. K.M.A. helped design, analyze, and interpret all experiments. L.J.S. and K.M.A. wrote the manuscript. All authors reviewed and approved the manuscript.

Asthma is a respiratory disorder characterized by reversible airflow limitation, bronchial hyperresponsiveness, and airway inflammation[1,2]. Although it is clear that asthma is a heterogeneous syndrome, a prominent subset of asthma is characterized by type 2 inflammation with infiltration of T helper type 2 (T_H2) cells to the airways and lung parenchyma, and a molecular signature of airway epithelial cell exposure to T_H2 cytokines, especially interleukin 13(IL-13) (ref. 3,4). IL-13 coordinates allergic lung inflammation through receptors on both structural and inflammatory cells. It induces epithelial cell hyperplasia and mucus production, airway smooth muscle cell hyperresponsiveness, and the recruitment and survival of eosinophils, which is enhanced by another T_H2 cytokine, IL-5 (ref. 5). IL-13 is a key driver of airway inflammation in mouse models of asthma [6], and biomarkers of type 2 inflammation predict enhanced clinical benefit from treatment with antibodies that block IL-13 signaling such as lebrikizumab [7] and dupilumab [8].

The external signals and transcription factors that regulate T_H2 cell differentiation are well understood. The cytokine IL-4 is both the canonical product of T_H2 cells and a powerful driver of T_H2 cell differentiation. Naive CD4 T cell precursors require concurrent T cell antigen receptor (TCR) and cytokine signals to induce T_H2 differentiation. TCR ligation activates T cells through a broad signaling cascade that includes the PI(3)K and NF-κB pathways. IL-4 receptor signals activate STAT6, which upregulates GATA-3 in activated T cells. Together these two key transcription factors promote T_H2 cell differentiation and cytokine production [9]. Because T_H2 cell differentiation is governed by a cytokine and transcription factor positive feedback loop, it is very sensitive to minor changes in cytokine production, the strength of TCR stimulation, and other intrinsic and environmental factors. Our extensive knowledge of the signals that control T cell differentiation and our ability to reproducibly manipulate this process *in vitro* make it an attractive system for the study of basic principles that govern gene expression networks and cell identity.

MicroRNAs (miRNAs) regulate gene expression programs by reducing the translation and stability of target mRNAs [10]. miRNAs are grouped into families that share a network of predicted mRNA targets. Although the quantitative effect produced by each miRNA-target interaction is small, the combined effect of the network of miRNA-target interactions produces substantial changes in cell behavior. Several studies have attempted to understand miRNA functions in asthma by analyzing miRNA expression in whole lung, airway epithelial cells, or mixed peripheral blood lymphocytes from humans with asthma or mice subjected to allergic airway inflammation models [11-14]. These studies provide insight into the effect of airway inflammation on miRNA expression patterns, but they do not define cell-intrinsic effects of miRNA regulation on disease pathogenesis.

In T cells, miRNAs regulate proliferation, survival, activation, differentiation, and cytokine production [15]. The miR-17∼92 cluster has emerged as a particularly potent and pleiotropic regulator of T cell responses. This cluster is transcribed as a single primary miRNA transcript that is processed to produce six mature miRNAs belonging to four miRNA families: miR-17, miR-18, miR-19, and miR-92 families [16]. Primary miR-17∼92 and the corresponding mature miRNAs are upregulated in activated CD4 T cells and can promote T cell proliferation and survival [17-20]. Although they are expressed without apparent cell-type specificity, miRNAs in the miR-17∼92 cluster regulate the differentiation and function of

several distinct T cell subsets. Both miR-17 and miR-19b promote T_H1 and T_H17 cell differentiation [18,21]. These two miRNAs also inhibit inducible T_{reg} cell differentiation *in vitro* [18], but the cluster as a whole is required for normal T_{reg} cell function *in vivo* [22]. T_{FH} cell responses are reduced and dysregulated in the absence of miR-17∼92[23,24]. However, miRNA regulation of T_H2 cell differentiation and cytokine production remains poorly understood.

We hypothesized that miRNAs that are differentially expressed in airway-infiltrating T cells in asthma regulate T_H2 cell function and promote lung inflammation. We used a highly sensitive nanoscale microfluidic qPCR approach to profile miRNA expression in $CD4^+$ T cells isolated from human asthmatic airways[25,26]. miR-19a, a member of the miR-17∼92 cluster, was significantly upregulated in asthma. Using genetically engineered mice, we found that miR-17∼92 promotes T_H2 cytokine production *in vitro* and type 2 inflammation *in vivo*. We mapped miR-17∼92 regulation of T_H2 cytokine production to the miR-19 family using transfectable miRNA mimics and inhibitors in primary human and mouse T cells. A functional screen of the miR-19 target network in T_H2 cells revealed several signaling inhibitors that restrain IL-13 and IL-4 production. Taken together, our data indicate that the observed increase in T cell miR-19a expression in humans with asthma augments T_H2 responses in their airways.

Results

miRNA expression in airway CD4 T cells

To investigate miRNA expression in airway-infiltrating T cells, we profiled the expression of a panel of 190 miRNAs in $CD4^+$ T cells sorted from bronchoalveolar lavage (BAL) fluid from 8 healthy, 13 steroid-naive asthmatic, and 21 steroid-using asthmatic subjects (Table 1)[12]. RNA was extracted from sorted $CD3^+$ $CD4^+$ T cells, and miRNA expression was determined by nanoscale microfluidic qPCR on 100 pg RNA from each subject (Supplementary Fig. 1a, Supplementary Table 1). Our analysis revealed few differences in miRNA expression between asthmatic and healthy $CD4^+$ T cells from BAL with one notable exception (Supplementary Fig. 1b, Supplementary Table 2). Of the 89 miRNAs that were detected in at least 60% of the subjects, miRNA-19a was the most significantly elevated in asthma (Fig. 1a, Supplementary Table 2 $p = 0.0199$). miR-19a expression was consistently elevated in all of the steroid-naive asthmatic subjects with very little variability, and was similarly elevated in the steroid-using asthmatic subjects that were treated with the inhaled corticosteroid (ICS) budesonide (Fig. 1c). This miRNA remained elevated in $CD4^+$ T cells from steroid-naive asthmatics upon 6 weeks of ICS treatment (Fig. 1d), indicating that it is resistant to gene expression changes induced by steroid treatment. Because miR-19a is a member of the miR-17∼92 cluster, a highly conserved cluster of 6 miRNAs transcribed in one polycistronic pri-miRNA, we investigated the expression of other members of the cluster. Only miR-19a, and not miR-19b, miR-17, miR-18a, or miR-20a, was differentially expressed between asthmatic and healthy $CD4^+$ T cells (Fig. 1e). These data demonstrate that miR-19a is specifically elevated in airway T cells in asthma, and indicate that individual members of the miR-17∼92 cluster are differentially regulated in this setting.

miR-17~92 promotes T_H2 cytokine production

The miR-17∼92 cluster regulates the differentiation and effector functions of several helper T cell subsets including T_H1, T_H17, T_{FH} and T_{reg} cells with varying degrees of potency [19-24]. However, the cluster's role in T_H2 cell differentiation and cytokine production, important features of the asthmatic immune response, has not been investigated. To this end, we cultured miR-17∼92-deficient $CD4^+$ T cells (called '$17{\sim}92^{\Delta/\Delta}$' here), miR-17∼92-sufficient control $CD4^+$ T cells (called $17{\sim}92^{+/+}$ here), and transgenic miR-17∼92-overexpressing $CD4^+$ T cells (called $17{\sim}92^{GFP/+}$ here) in T_H2 polarizing conditions. Intracellular cytokine staining revealed that $17{\sim}92^{GFP/+}$ cells produced more of the type 2 cytokine IL-13 compared to $17{\sim}92^{+/+}$ controls (Fig. 2a). Conversely, fewer $17{\sim}92^{\Delta/\Delta}$ cells produced the type 2 cytokines IL-13, IL-5, and IL-4 compared to $17{\sim}92^{+/+}$ controls (Fig. 2a-b). This defect in T_H2 differentiation and cytokine production did not result in increased T_H1 cytokine production, as measured by IFN-γ production (Fig. 2c). $17{\sim}92^{\Delta/\Delta}$ cells produced substantially more TNF, which is a known direct target of miR-19 (Fig. 2c), suggesting that these cells are capable of efficient cytokine production in T_H2-polarizing conditions, and that the defect is limited to type 2 cytokines. $17{\sim}92^{\Delta/\Delta}$ cells produced less T_H2 cytokines even in established GATA-3^{hi} T_H2 cells (Fig. 2d). Thus, the miR-17∼92 cluster positively regulates T_H2 cytokine production.

To determine whether the T_H2 cytokine defect was cell-intrinsic, we co-cultured congenically marked $17{\sim}92^{\Delta/\Delta}$ and $17{\sim}92^{+/+}$ $CD4^+$ T cells in T_H2 conditions. After 5 days in culture, the $CD45.1^+$ $17{\sim}92^{\Delta/\Delta}$ T cells produced less IL-13 and IL-4 compared to the $CD45.2^+$ $17{\sim}92^{+/+}$ cells (Fig. 3a), demonstrating that the cytokine defect is cell-intrinsic and does not entirely depend on feedback from IL-4 or other products produced by the mutant T cells in culture.

We observed a slight proliferation defect in $17{\sim}92^{\Delta/\Delta}$ T_H2 cell cultures compared to $17{\sim}92^{+/+}$ controls, and a slight increase in proliferation in $17{\sim}92^{GFP/+}$ cells (Fig. 3b). To test whether the frequency of T_H2 cytokine-producing cells among $17{\sim}92^{\Delta/\Delta}$, $17{\sim}92^{+/+}$, and $17{\sim}92^{GFP/+}$ $CD4^+$ T cells was an indirect result of their rate of proliferation, we labeled the cells with Cell Trace Violet (CTV) and analyzed cytokine production at each division after 5 days of culture in T_H2 polarizing conditions. IL-13 and IL-5 production did increase with each cell division in $17{\sim}92^{+/+}$ cells. However, $17{\sim}92^{\Delta/\Delta}$ cells produced significantly less IL-13, IL-5, and IL-4 at each cell division compared to $17{\sim}92^{+/+}$ cells (Fig. 3c, d). In contrast, $17{\sim}92^{GFP/+}$ cells produced more IL-13 and IL-5 at each division, but an equal amount of IL-4 as compared to $17{\sim}92^{+/+}$ cells (Fig. 3c, d). Together these data indicate that the miR-17∼92 cluster promotes type 2 cytokine production in a cell-intrinsic and proliferation-independent manner.

miR-19 augments T_H2 differentiation

To understand the mechanism of miR-17∼92 control of T_H2 cell cytokine production, the functions of individual miRNA members of the cluster need to be addressed. Therefore, we transfected mature miRNA mimics corresponding to each of the six miRNAs in the miR-17∼92 cluster into $17{\sim}92^{\Delta/\Delta}$ $CD4^+$ T cells on days 1 and 4 of T_H2 polarizing cultures. Transfection of either miR-19a or miR-19b was sufficient to completely rescue T_H2

cytokine production (Fig. 4a-c). Other miRNAs within the cluster conferred only partial rescue of T_H2 cytokine production compared to miR-19a or miR-19b. These data indicate that miR-19 is the primary component of the miR-17∼92 cluster that augments T_H2 differentiation.

All of the miR-19a and the large majority of miR-19b expressed in T cells derive from the miR-17∼92 cluster (Supplementary Fig. 2). Consistent with this finding, specific retroviral sensors of miR-19a and miR-19b activity were strongly repressed in $17{\sim}92^{+/+}$ cells, but not $17{\sim}92^{\Delta/\Delta}$ cells (Supplementary Fig. 3). T cell activation induces increased transcription of the miR-17∼92 cluster, and all of the miRNAs in the cluster remain highly expressed during T_H2 cell differentiation[27] (and data not shown). A single transfection either early in the culture (day 1) or late (day 4) did not rescue T_H2 cytokine production (Fig. 4d, e). We conclude that miR-19 is required throughout T_H2 cell polarization to support robust T_H2 cell differentiation and cytokine production. miR-19 mimics also modestly increased proliferation of $17{\sim}92^{\Delta/\Delta}$ cells in T_H2 conditions (Supplementary Fig. 4).

We next tested whether modulating the activity of miR-19 alone was sufficient to alter type 2 cytokine production in miR-17∼92-sufficient T cells with normal endogenous expression of the other miRNAs in the cluster. Transfection of miR-19a and miR-19b inhibitors into $17{\sim}92^{+/+}$ T cells specifically increased the expression of corresponding GFP sensors of miR-19a and miR-19b activity and decreased expression of IL-13 (Supplementary Fig. 3). These inhibitors also significantly reduced IL-13, but not IL-4, production when transfected into human cord blood $CD4^+$ T cells in T_H2-polarizing cultures (Fig. 5a, b). Conversely, transfection with miR-19a mimic was sufficient to increase IL-13 expression, but not IL-4, in human cord blood $CD4^+$ T cells (Fig. 5c, d). Similarly, $17{\sim}92^{+/+}$ mouse CD4 T cells had increased IL-13 production, but not IL-4, when transfected with miR-19a or miR-19b mimics in non-polarizing conditions (Supplementary Fig. 3). We conclude that changes in miR-19 expression, such as those seen in human asthmatic airway T cells, are sufficient to modulate the abundance of IL-13 produced in primary human and mouse $CD4^+$ T cells.

miR-19 targets *Pten*, *Socs1*, and *Tnfaip3*

Because a large number of direct miR-19 targets have been validated in B cell lymphomas and other cell types, we took a candidate approach to uncover how miR-19 augments T_H2 differentiation. We individually inhibited the 38 previously validated [28-30] miR-19 targets that are expressed in T cells[31] with siRNA SmartPools in $17{\sim}92^{\Delta/\Delta}$ $CD4^+$ T cells during T_H2 polarization (Supplementary Table 3). IL-13 and IL-4 *z*-scores were calculated for each of the transfections (Fig. 6a, b). The top 8 candidate genes that when inhibited increased IL-13 and IL-4 were characterized further by inhibition with 3 individual siRNAs per gene in $17{\sim}92^{\Delta/\Delta}$ $CD4^+$ T cells during T_H2 polarization to confirm the rescue of IL-13 and IL-4 (Fig. 6c, d). The type 2 cytokine defect of $17{\sim}92^{\Delta/\Delta}$ cells was rescued by inhibition of *Pten*, *Socs1*, and *Tnfaip3* (which encodes A20) with at least 2 out of 3 individual siRNAs (Fig. 6e). Each of the top 8 candidate genes was confirmed to be inhibited by miR-19 expression by qPCR of $17{\sim}92^{\Delta/\Delta}$ cells transfected with miR-19a, -19b, or control mimics, compared to $17{\sim}92^{+/+}$ cells (Fig. 6f). Furthermore, to test whether genetic depletion of PTEN expression in $17{\sim}92^{\Delta/\Delta}$ cells could rescue T_H2 cytokine production, we deleted one allele of *Pten* in

17∼92$^{\Delta/\Delta}$ cells (17∼92$^{\Delta/\Delta}$ *Pten*$^{\Delta/+}$). Genetic depletion of PTEN moderately rescued the cytokine defect of 17∼92$^{\Delta/\Delta}$ T cells (Fig. 6g).

Pten, *Socs1*, and *Tnfaip3* are negative regulators of T cell signaling pathways that are important for all T helper cell subsets. To test whether each of these targets regulated other T helper cell cytokines, such as IFN-γ, IL-17A, and IL-17F, we transfected 17∼92$^{\Delta/\Delta}$ cells with individual siRNAs against *Pten*, *Socs1*, and *Tnfaip3* under non-polarizing (T_HN), T_H17, and T_H2-polarizing conditions (Fig. 6h-j). Consistent with previous reports [18,21], *Pten* inhibition increased the production of all T helper cytokines tested, but reducing *Socs1* or *Tnfaip3* expression enhanced production of T_H2 cytokines, but not IFN-γ or IL-17. Thus, miR-19 specifically regulates T_H2 responses through distinct limiting mRNA targets.

miR-17~92 augments T_H2 cell function *in vivo*

We next tested whether reduced T_H2 cytokine production by 17∼92$^{\Delta/\Delta}$ T cells would result in altered airway type 2 inflammation *in vivo*. We transferred 17∼92$^{\Delta/\Delta}$ or 17∼92$^{+/+}$ ovalbumin (OVA)-specific OT-II T_H2 cells to *Cd28*$^{-/-}$ mice, and challenged the mice every 24 h oropharyngeally with OVA for 3 days (Supplementary Fig. 5a). 18 h after the last challenge, we analyzed pulmonary resistance in response to increasing doses of acetylcholine. Mice that received either no OT-II cells or 17∼92$^{\Delta/\Delta}$ OT-II T_H2 cells had significantly lower pulmonary resistance than mice that received 17∼92$^{+/+}$ OT-II T_H2 cells (Fig. 7a), indicating that T_H2 cells that lack the miR-17∼92 cluster are less capable of inducing allergic airway hyperresponsiveness. Histological analysis of lung sections from these mice revealed increased mucus-secreting goblet cells and more severe inflammation in mice that received 17∼92$^{+/+}$ OT-II T_H2 cells compared to those that received 17∼92$^{\Delta/\Delta}$ OT-II T_H2 cells (Fig. 7b-d). Mice that received 17∼92$^{\Delta/\Delta}$ OT-II T_H2 cells transfected with miR-19a mimic showed a trend toward increased inflammation and mucus secretion (Fig. 7b-d). To better characterize and quantify airway inflammation, we analyzed BAL from the recipient mice by flow cytometry (Supplementary Fig. 5b). Mice that received 17∼92$^{\Delta/\Delta}$ OT-II T_H2 cells had significantly reduced eosinophilia in the airways compared to mice that received 17∼92$^{+/+}$ OT-II T_H2 cells (Fig. 7e). However, 17∼92$^{\Delta/\Delta}$ OT-II T_H2 cells transfected with miR-19a induced airway eosinophil infiltration similar to that seen in recipients of 17∼92$^{+/+}$ OT-II T_H2 cells (Fig. 7e). Macrophage and neutrophil numbers were relatively similar in all three groups of recipients, suggesting that the differences in airway inflammation were restricted to effects induced by type 2 cytokines. We conclude that the miR-17∼92 cluster, and miR-19a specifically, has a role in the *in vivo* function of T_H2 cells as inducers of the allergic inflammatory phenotype associated with asthma.

Discussion

Guided by miRNA expression in T cells present in the airways in human asthma, we identified a miRNA that augments T_H2 cytokine production and allergic inflammation via coordinate regulation of cytokine and antigen receptor signaling pathways. Our data demonstrate that the miR-17∼92 cluster, and specifically miR-19a, promotes T_H2 cytokine production by simultaneously targeting inhibitors of the NF-κB, JAK-STAT, and PI(3)K pathways. In the context of previous studies of the miR-17∼92 cluster, these findings

illustrate basic principles of miRNA regulation, including the network logic of miRNA function, and how complex biological processes such as effective T cell-mediated immune responses emerge from coordinate miRNA regulation of diverse aspects of cell behavior.

The miR-17∼92 cluster has many established functions in lymphocytes[32]. The cluster as a whole promotes T cell proliferation and survival, and the differentiation and function of several committed effector T cell subsets[18,19,21-24], making it an important coordinator of T cell responses. T_{FH} responses involve the concerted action of all 4 miRNA families in the miR-17∼92 cluster[23,24]. miR-17 and miR-92 family miRNAs support T cell proliferation in the absence of other miRNAs[20]. In our experiments, miR-19 as well as miR-17 and miR-92 family miRNAs partially rescued $17{\sim}92^{\Delta/\Delta}$ T cell proliferation. Both miR-17 and miR-19b promote T cell survival and T_H1 and T_H17 cell differentiation, while limiting iT_{reg} cell differentiation [18,21]. However, no specific functions have previously been attributed to miR-19a in T helper cells. We mapped the T_H2 cytokine-promoting activity of the miR-17∼92 cluster to miR-19, as both miR-19a and miR-19b (but not other miRNAs in the cluster) rescued IL-13 and IL-4 production in $17{\sim}92^{\Delta/\Delta}$ T cells.

Our study emphasizes an important concept regarding the mechanism of miRNA regulation of cell behavior: a single miRNA can be expressed in and regulate many different cell types through distinct but overlapping networks of targets. Each target may play a limiting role in distinct differentiation environments, or may play a similar role in a variety of contexts. For example, miR-19 regulated T_H2 cytokine production in part through PTEN, a target that has widespread effects on T helper cell effector programs [18,19,21,23]. In contrast, SOCS1 and A20 were limiting factors for T_H2, but not T_H1 or T_H17 cytokine production. The same concept applies to transcription factors and their target genes. For example, c-Maf regulates both T_H2 and T_H17 cytokine production through distinct molecular pathways. Similarly, GATA-3 is the principle determinant of T_H2 cell differentiation and a direct regulator of *Il13* and *Il5,* but it also regulates T cell development in the thymus and survival in the periphery. Our findings demonstrate that careful dissection of target networks can reveal not only the mechanisms through which transcription factors and miRNAs mediate their functions, but also novel or unexpected limiting requirements for downstream genes and pathways that coordinate T cell-mediated immunity.

We identified at least three important pieces of the miR-19 target network in T_H2 cells: *Pten*, *Socs1,* and *Tnfaip3*. Each of these target mRNAs encodes an inhibitor of a distinct signaling pathway, indicating that miR-19 augments T_H2 cytokine production by simultaneously amplifying PI(3)K, JAK-STAT, and NF-κB signaling. However, our analysis revealed a limiting independent role for each target, since depleting each one individually was sufficient to markedly increase T_H2 cytokine production. These pathways are all essential components of the antigen and cytokine signaling that induce T cell differentiation and effector function. As such, the importance of PTEN, SOCS1, and A20 for T_H2 cytokine production have been inferred or assumed, but never tested.

PTEN inhibits the PI(3)K pathway, which promotes T cell proliferation and cell survival[33], and deletion of one allele of *Pten* results in autoimmunity and lymphoproliferative disease in mice[34]. PTEN is an important miR-17∼92 target in T_H1, T_H17 and T_{FH} cell

differentiation[18,21,23,24], but its effects on cytokine production by T_H2 cells were previously unknown. Genetic rescue of PTEN over expression in 17∼92$^{\Delta/\Delta}$ cells partially rescued T_H2 cytokine production, indicating that both PTEN and other targets significantly contribute to the T_H2 phenotype.

SOCS1 inhibits the JAK-STAT pathway downstream of cytokine receptors[35], and favors T_H17 over T_H1 differentiation by repressing IL-12 and IFN-γ signaling[36,37]. Both IFN-γ and IL-4-producing CD4$^+$ T cells are increased in SOCS1-deficient mice[38] and SOCS1 inhibits IL-4 signaling in macrophages[39]. These findings have led to speculation that SOCS1 may inhibit T_H2 responses[40], but this possibility had remained untested prior to our experiments. Furthermore, SOCS1 has not previously been found to be an important miR-17∼92 target in regulating the differentiation and effector functions of any helper T cell subset.

Tnfaip3 encodes A20, a constitutively expressed negative regulator of the NF-κB pathway in T cells. A20 was identified as an important miR-19 target in macrophages[30]. Inhibition of A20 increases IL-2 production in Jurkat cells[41], but its effect on T_H2 cytokine production had not yet been described. While identification of these three targets leads to better understanding of the intracellular components that regulate Th2 cytokine production, genome-wide approaches to determine the full miR-19 target network in T_H2 cells would likely reveal additional targets involved in helper T cell biology.

We hypothesized that miRNA expression profiling in airway-infiltrating T cells could reveal functionally relevant miRNAs and pathways that are directly involved in asthma pathogenesis. Indeed, we identified miR-19a as a candidate regulator of T_H2 responses through miRNA profiling[25,26] in the small number of CD4 T cells that can be recovered from bronchoalveolar lavage. Previous studies identified miRNAs of interest by profiling expression in complex cell mixtures, such as whole lungs in animal models[14], epithelial cell brushings[12], or mixed lymphocytes from peripheral blood of asthmatic subjects[11,42]. Interpretation of data from unseparated tissues can be ambiguous. Differential miRNA expression may reflect changes in cellular composition of samples from asthmatic subjects, and formation of mechanistic hypotheses about disease pathogenesis requires further work to identify which cell type(s) exhibit differential expression of any miRNA of interest. Future studies will be needed to confirm the observed increase in miR-19a in airway CD4$^+$ T cells in asthma, and to determine whether this change is limited to T_H2 cells in this context. Larger studies may also identify correlation between miR-19a expression and asthma severity, lung function, response to corticosteroid treatment, or biomarkers of T_H2 inflammation that stratify asthma phenotypes[1,43].

Although clusters of miRNAs are transcribed as a single polycistronic primary miRNA (pri-miRNA) transcript, each mature miRNA in the cluster is not necessarily expressed at the same abundance in a given cell type and condition. Nevertheless, we were surprised to find a specific increase in miR-19a, but not other members of the miR-17∼92 cluster, in airway-infiltrating T cells in asthma. miR-19a and miR-19b were also preferentially increased in premalignant cells in a mouse model of B cell lymphoma and in human Burkitt's lymphoma cell lines[16]. A specific increase in miR-19a may be mediated by preferential processing from the polycistronic miR-17∼92 pri-miRNA transcript, or by a sequence-specific increase in

the efficiency of some other step in miR-19a biogenesis. Alternatively, mature miR-19a may be specifically stabilized in T cells in inflamed lungs. Regardless of the mechanism, the observed increase in miR-19a abundance should have a significant impact on secretion of IL-13, since altering miR-19a activity by over expression or depletion in both human and mouse primary T cells altered IL-13 production *in vitro*.

The identity and function of miRNAs that regulate type 2 inflammation in a T cell-intrinsic manner have remained uncertain. miR-155 has been a major focus because miR-155-deficient T cells have a modest bias toward T_H2 differentiation *in vitro*[44,45] and miR-155-deficient mice develop partially penetrant spontaneous airway remodeling with some of the characteristics of asthma[44]. However, these mice are resistant to experimentally induced airway inflammation[46], suggesting that miR-155 may have a role in cell types other than T_H2 cells in this model. Our data suggest that miR-19a upregulation in T cells in asthmatic airways may be an indicator and a cause of increased IL-13 production, and likely contributes to type 2 inflammation in asthma. Indeed, $17{\sim}92^{\Delta/\Delta}$ T_H2 cells induced far less airway eosinophiliathan $17{\sim}92^{+/+}$ T_H2 cells in an allergic airway inflammation model, and restoration of miR-19a was sufficient to rescue this defect.

Our study links miR-19a activity with human asthma and uncovers mechanisms of miR-19a function in T cells, suggesting that miR-19 may be an attractive drug target. Previous animal model studies have validated the concept of miRNA-based therapy by using intranasal administration of sequence-specific miRNA inhibitors to ameliorate allergic airway inflammation[13,47-49]. In addition, uncovering the target networks through which miRNAs act may be an effective path to the development of novel therapies. For example, our findings lend weight to the argument that NF-κB inhibitors might be effective in asthma and other allergic diseases[50]. Through coordinate repression of several mRNA targets, miR-19 amplifies signals that augment production of T_H2 cytokines, the principle drivers of asthma pathogenesis.

Online Methods

Human subjects

Bronchoalveolar lavage (BAL) fluid was obtained from three groups of subjects: asthmatic subjects that had not been treated with inhaled corticosteroids (ICS) for 6 weeks prior to the study start date, called “steroid-naive” here; asthmatic subjects that were treated continuously with ICS, called “steroid-using” here, and healthy control subjects. BAL was obtained from steroid-naïve subjects at baseline and again after 8 weeks of ICS treatment, 200μg budesonide twice a day. BAL was obtained from steroid-using subjects after standardizing their ICS treatment to a regimen of 200μg budesonide twice a day for 8 weeks. This study, called the Study of the Mechanisms of Asthma (MAST), was registered on clinicaltrials.gov: NCT00595153. A power calculation was used to determine the number of subjects needed to measure differences in expression of 3 biomarker genes of IL-13 exposure in the airway. We utilized all sorted T cell samples available from this completed study. Inclusion and exclusion criteria for human subjects are provided on clinicaltrials.gov. Written informed consent was obtained from all subjects, and all studies were performed with approval from the UCSF Committee on Human Research.

Sorting of clinical BAL samples

Investigators were blinded to the group allocation of subjects during cell sorting and sample processing. Live $CD3^+$ $CD4^+$ T cells were sorted using a FACSAria flow cytometer (BD Biosciences, San Jose, CA) from BAL cells transported in ice cold PBS with 5% FCS within approximately four hours of collection. CD3-PE (cat# MHCD03044) was purchased from Invitrogen (Carlsbad, CA). CD4-Cy7 (cat# 557852), CD8-APC-Cy7 (cat# 557834), and PI (cat# 51-66211E) were purchased from BD Biosciences (San Jose, CA). The average purity of the sorted cells, confirmed by flow cytometric analysis, exceeded 95%. Sorted cells were washed in ice cold PBS with 2% FCS and 2 mM EDTA and then lysed in RLT buffer (Qiagen, Valencia, CA) prior to being snap-frozen and stored at -80°C.

High-throughput multiplex qPCR

High-throughput multiplex qPCR was performed according to a previously described protocol[26]. Briefly, CD4 T cells sorted by flow cytometry from clinical samples were lysed and stored in RLT buffer (Qiagen) at -80°C until all samples were collected. Frozen lysates were thawed and loaded onto QIAshredder homogenizer columns (Qiagen). Using a low concentration of ethanol (35% v/v), the large fraction of RNA (>150nt) was precipitated and captured on collection columns (RNeasy, Qiagen). The small fraction of RNA (<150nt) does not bind with low concentration of RNA, and so the flow-through from the first column was brought up to a concentration of 75% v/v ethanol and RNA was precipitated and collected on a fresh column (MinElute, Qiagen). Both RNA fractions were treated with DNase per manufacturer's recommendations (Qiagen). 2μl of RNA from each large fraction, as well as a standard curve of RNA from *in vitro*-derived T_H2 cells, were reverse transcribed using the SuperScript III kit (Invitrogen). RNA was then quantified by qPCR using primers for *β2m* and comparing to the standard curve of RNA. We calculated 100pg RNA from the small fraction for each sample for multiplex reverse transcription using 2 separate mixes of 96 miRNA stem loop reverse primers at a final concentration of 1 nM (Supplemental table 1). Reverse transcription and 20 cycles of preamplification were performed according to previous protocols[25,26]. Excess primers were removed from samples using 9μl ExoSAP-IT (USB) per sample, and then 15μl of each sample was purified on Illustra AutoScreen-96 Well Plates (GE Healthcare). MiRNA qPCR data was collected on the BioMark system (Fluidigm) using a 96.96 Dynamic Array Integrated Fluidic Circuit (IFC).

Fluidigm Biomark qPCR data analysis

Data was first analyzed on Real Time PCR Analysis software (Fluidigm) with the quality threshold set at 0.5, baseline correction set to linear (derivative), and Ct threshold method set to auto (detectors). The data was further analyzed in R (version 2.14.1) through the following pipeline: Ct values < 5 or >28 were removed per Fluidigm recommendations: miRNAs that were detected in less than 60% of patient samples were removed from analysis; missing Ct values were replaced with the limit of detection (highest Ct value within the standard curve) + 0.1, and 4) the data were global mean-normalized per plate to account for inter-plate differences.

Mice

Mice with *lox*P-flanked alleles encoding miR-17∼92 (*Mirc1*$^{fl/fl}$, 008458, The Jackson Laboratory), and *Rosa26*-miR-17∼92–transgenic mice (Gt(ROSA)26Sor$^{tm3(CAG-MIR17-92,-EGFP)Rsky}$, 008517, The Jackson Laboratory) were crossed to CD4-Cre mice (4196, Taconic) to generate CD4-Cre; *Mirc1*$^{fl/fl}$ (called '17∼92$^{\Delta/\Delta}$' here), CD4-Cre;Gt(ROSA)26Sor$^{tm3(CAG-MIR17-92,-EGFP)Rsky}$ (called '17∼92$^{GFP/+}$' here), and CD4-Cre; *Mirc1*$^{+/+}$ or *Mirc1*$^{fl/fl}$; (collectively called '17∼92$^{+/+}$' here). OT-II mice (004194), and mice heterozygous for the *Rora*^{sg} mutation (002651) were from The Jackson Laboratory. Mice with *lox*P-flanked *Pten* alleles have been described[51]. *Cd28*$^{-/-}$ mice (002666) were from The Jackson Laboratory. All mice were housed and bred in the specific pathogen-free barrier facility at the University of California, San Francisco. The Institutional Animal Care and Use Committee at the University of California, San Francisco, approved all animal experiments.

In vitro human cord blood T cell polarization

Peripheral blood mononuclear cells (PBMCs) from anonymous human cord blood donors were isolated by Lymphoprep gradient (Accurate Chemical & Scientific Corp; cat # 1114545). CD4$^+$ T cells were isolated from PBMCs using the Dynabeads Untouched Human CD4$^+$ T Cell Isolation Kit (Invitrogen). Cells were stimulated for ∼65 h on plates coated with 1μg/ml anti-CD3 (UCSF Monoclonal Antibody Core; clone OKT-3) and 2μg/ml anti-CD28 (UCSF Monoclonal Antibody Core; clone 9.3) at an initial density of 0.7×10^6 cells/ml. After stimulation, the cells were rested for two days in media containing 20 units/ml recombinant human IL-2 (NCI). For T_H2 polarizing conditions, 12.5 ng/ml recombinant human IL-4 (PeproTech; cat # 200-04) was added throughout the 5 days. T cell culture was in RPMI-1640 media with 10% FCS, pyruvate, nonessential amino acids, L-arginine, L-asparagine, L-glutamine, folic acid, beta mercaptoethanol, penicillin, and streptomycin.

In vitro mouse primary T cell polarization

CD4$^+$ T cells were isolated from spleen and lymph nodes of young mice (4-8 weeks old) using the Mouse CD4 Dynabeads Isolation kit (Invitrogen; L3T4). For experiments including Cell Trace Violet (Invitrogen), cells were stained at 5μM in PBS for 20 minutes at 37°C, quenched with 5 volumes of media with 10% FCS for 5 minutes, and washed twice in media prior to culture. For all conditions, cells were activated with hamster anti-mouse anti-CD3 (clone 2C11, 0.25μg/ml) and anti-mouse CD28 (clone 37.51, 1μg/ml) antibodies on a plate coated with goat anti-hamster IgG (0.3 mg/ml in PBS; MP Biomedicals) for ∼65 h at an initial density of 0.7×10^6 cells/ml, and then rested in media with 20 units/ml recombinant IL-2 (National Cancer Institute) for 48-72 h. For T_H2 polarizing conditions, 500 units/ml IL-4 supernatant and 5μg/ml anti-IFN-γ(clone XMG1.2) were added to the culture throughout the 5-6 days. "Low T_H2" conditions included only 5 units/ml IL-4, and "T_HN" conditions received no polarizing cytokines or antibodies. T_H17 polarizing conditions received 5ng/ml recombinant human TGF-β (Peprotech), 25ng/ml recombinant murine IL-6 (Peprotech), 10ug/ml anti-IL-4 (clone 11B11), 10ug/ml anti-IFN-g, and 20ng/ml recombinant murine IL-23 (R&D Systems) throughout the 5 days of culture. All cultures

used DMEM high glucose media supplemented with 10% FCS, pyruvate, nonessential amino acids, MEM vitamins, L-arginine, L-asparagine, L-glutamine, folic acid, beta mercaptoethanol, penicillin, and streptomycin.

miRNA mimics, miRNA inhibitors, siRNA, and miRNA sensors

During *in vitro* polarization, human or mouse primary $CD4^+$ T cells in culture were transfected with miRNA mimics, inhibitors, or siRNAs (Dharmacon) at 24 and 96 h of culture. miRIDIAN miRNA mimics were used at 500nM per transfection. miRIDIAN miRNA Hairpin Inhibitors were also used at 500 nM. siGENOME SmartPools and ON-TARGET plus Individual siRNA were used at 500 nM. Cells were transfected using the Neon Transfection system by Invitrogen as described[20]. Retroviral miRNA sensors containing 4 perfectly complementary binding sites for miR-1, miR-19a, and miR-19b were constructed and transduced at 48 h as described[20].

Intracellular cytokine and transcription factors stains

For cytokine staining, cells were restimulated with 20 nM PMA and 1μM ionomycin for 4 hours, and 5μg/ml brefeldin A was added during the last 2 hours of restimulation. Cells were stained with the viability dye eFluor780 (eBiosciences; Cat # 65-0865-14), and then fixed in 4% paraformaldehyde for 8 minutes at room temperature. Cytokine staining was done in permeabilization buffer containing 0.05% saponin. For transcription factor staining, unstimulated cells were fixed, permeabilized, and stained using the FoxP3 Staining Kit (eBiosciences; Cat # 00-5523-00). Samples were analyzed with a flow cytometer (BD LSR II). Mouse antibodies: IL-13-PE (eBiosciences; eBio13A), IL-4-APC (eBiosciences; 11B11), IL-5-PE (Biolegend; TRFK5), IFNg-FITC (eBiosciences; XMG1.2), TNFa-AlexaFluor700 (BD Biosciences; MP6-XT22), and GATA-3-PE (eBiosciences; E50-2440). Human antibodies: IL-13-FITC (eBiosciences; PVM13-1), IL-4-APC (BD Biosciences; 8D4-8), IL-17A-eFluor450 (eBiosciences; eBio17B7), and IL-17F-PE (BD Pharmingen; 079-289).

In vivo allergic airway inflammation model

For each *in vivo* experiment, we used at least 5 mice per group to gain power for statistical analysis, and repeated the model to pool data and determine reproducibility. Mice received 3 different cell types in rotation such that each cage had 1-2 recipients for each cell type. Mice were challenged in random order and were tested for pulmonary resistance in rotating order through each group. One mouse was removed from analysis due to low body weight and lack of movement; histological analysis confirmed signs of emphysema. Six- to eight-week old sex-matched littermate *Cd28*$^{-/-}$ mice were injected retro-orbitally with 2×10^5 *in vitro* T_H2-polarized $17\sim92^{+/+}$ or $17\sim92^{\Delta/\Delta}$ OT-II cells. The mice were challenged oropharyngeally with 50μg ovalbumin (OVA) in PBS at 24, 48, and 72 hours post transfer to induce allergic airway inflammation. 18 hours after the final challenge, mice were anesthetized with ketamine/xyalazine, and pulmonary resistance was measured by trachaea cannulation in response to intravenous acetylcholine, as previously described [52]. BAL was collected by 5 lavages of 0.8 ml of PBS for flow cytometry, and lungs were filled with 10% buffered formalin and fixed for histology. BAL cells were washed, counted, and surface

stained for analysis by flow cytometry. Antibodies used for myeloid cell enumeration: CD11b-AlexaFluor488 (eBiosciences; M1/70), CD11c-PE-Cy7 (Biolegend; N418), Ly6G-V450 (BD Biosciences; 1A8), SiglecF-PE (BD Biosciences; E50-2440). Two paraffin-embedded 5 μm sections of the whole lung from each mouse were stained with H&E and PAS. To quantify inflammation, H&E-stained lung sections were de-identified for blinding and scored for peribronchial and perivascular inflammatory cell infiltration: grade 0, no infiltration; grade 1, <25% of examined area; grade 2, 25-50%; grade 3, 51-75%; and grade 4, >75%. To quantify goblet cell hyperplasia, PAS stained lung sections were de-identified for blinding and scored for the percentage of PAS positive cells among airway epithelial cells: grade 0: none; grade 1 <25% of airway epithelial cells; grade 2, 25-50%; grade 3, 51-75%; and grade 4, >75%.

Supplementary Material

Refer to Web version on PubMed Central for supplementary material.

Acknowledgments

This work was supported by the U.S. National Institutes of Health (HL107202, HL109102), the Sandler Asthma Basic Research Center, a Scholar Award from The Leukemia & Lymphoma Society, L.J.S. is a National Science Foundation predoctoral fellow (2010101500), the Swiss Foundation for Grants in Biology and Medicine (PASMP3-142725), the National Multiple Sclerosis Society, and the UCSF Program for Breakthrough Biomedical Research, which is funded in part by the Sandler Foundation. The authors would like to thank Mike McCune, Yelena Bronevetsky, and Elisabeth Krow-Lucal for help with human biospecimens, and Robin Kageyama for helpful discussion of the manuscript.

References

1. Wenzel SE. Asthma phenotypes: the evolution from clinical to molecular approaches. Nature Medicine. 2012; 18:716–725.
2. Locksley RM. Asthma and allergic inflammation. Cell. 2010; 140:777–783. [PubMed: 20303868]
3. Robinson DS, et al. Predominant TH2-like bronchoalveolar T-lymphocyte population in atopic asthma. N Engl J Med. 1992; 326:298–304. [PubMed: 1530827]
4. Woodruff PG, et al. T-helper Type 2–driven Inflammation Defines Major Subphenotypes of Asthma. Am J Respir Crit Care Med. 2009; 180:388–395. [PubMed: 19483109]
5. Wynn TA. IL-13 effector functions. Annu Rev Immunol. 2003; 21:425–456. [PubMed: 12615888]
6. Kuperman DA, et al. Direct effects of interleukin-13 on epithelial cells cause airway hyperreactivity and mucus overproduction in asthma. Nature Medicine. 2002; 8:885–889.
7. Corren J, et al. Lebrikizumab treatment in adults with asthma. N Engl J Med. 2011; 365:1088–1098. [PubMed: 21812663]
8. Wenzel S, et al. Dupilumab in persistent asthma with elevated eosinophil levels. N Engl J Med. 2013; 368:2455–2466. [PubMed: 23688323]
9. Ansel KM, Djuretic I, Tanasa B, Rao A. Regulation of Th2 differentiation and Il4 locus accessibility. Annu Rev Immunol. 2006; 24:607–656. [PubMed: 16551261]
10. Bartel DP. MicroRNAs: target recognition and regulatory functions. Cell. 2009; 136:215–233. [PubMed: 19167326]
11. Liu Y, Li H, Xiao T, Lu Q. Epigenetics in Immune-Mediated Pulmonary Diseases. Clinic Rev Allerg Immunol. 2013; 45:314–330.
12. Solberg OD, et al. Airway epithelial miRNA expression is altered in asthma. Am J Respir Crit Care Med. 2012; 186:965–974. [PubMed: 22955319]

13. Mattes J, Collison A, Plank M, Phipps S, Foster PS. Antagonism of microRNA-126 suppresses the effector function of TH2 cells and the development of allergic airways disease. Proc Natl Acad Sci USA. 2009; 106:18704–18709. [PubMed: 19843690]
14. Polikepahad S, et al. Proinflammatory role for let-7 microRNAS in experimental asthma. J Biol Chem. 2010; 285:30139–30149. [PubMed: 20630862]
15. Baumjohann D, Ansel KM. MicroRNA-mediated regulation of T helper cell differentiation and plasticity. Nat Rev Immunol. 2013; 13:666–678. [PubMed: 23907446]
16. Olive V, Li Q, He L. mir-17-92: a polycistronic oncomir with pleiotropic functions. Immunol Rev. 2013; 253:158–166. [PubMed: 23550645]
17. Bronevetsky Y, Ansel KM. Regulation of miRNA biogenesis and turnover in the immune system. Immunol Rev. 2013; 253:304–316. [PubMed: 23550654]
18. Jiang S, et al. Molecular dissection of the miR-17-92 cluster's critical dual roles in promoting Th1 responses and preventing inducible Treg differentiation. Blood. 2011; 118:5487–5497. [PubMed: 21972292]
19. Xiao C, et al. Lymphoproliferative disease and autoimmunity in mice with increased miR-17-92 expression in lymphocytes. Nat Immunol. 2008; 9:405–414. [PubMed: 18327259]
20. Steiner DF, et al. MicroRNA-29 regulates T-box transcription factors and interferon-γ production in helper T cells. Immunity. 2011; 35:169–181. [PubMed: 21820330]
21. Liu SQ, Jiang S, Li C, Zhang B, Li QJ. miR-17-92 cluster targets phosphatase and tensin homology and Ikaros Family Zinc Finger 4 to promote TH17-mediated inflammation. J Biol Chem. 2014; 289:12446–12456. [PubMed: 24644282]
22. de Kouchkovsky D, et al. microRNA-17-92 regulates IL-10 production by regulatory T cells and control of experimental autoimmune encephalomyelitis. J Immunol. 2013; 191:1594–1605. [PubMed: 23858035]
23. Baumjohann D, et al. The microRNA cluster miR-17∼92 promotes TFH cell differentiation and represses subset-inappropriate gene expression. Nat Immunol. 2013; 14:840–848. [PubMed: 23812098]
24. Kang SG, et al. MicroRNAs of the miR-17∼92 family are critical regulators of TFH differentiation. Nat Immunol. 2013; 14:849–857. [PubMed: 23812097]
25. Moltzahn F, et al. Microfluidic-based multiplex qRT-PCR identifies diagnostic and prognostic microRNA signatures in the sera of prostate cancer patients. Cancer Res. 2011; 71:550–560. [PubMed: 21098088]
26. Seumois G, et al. An integrated nano-scale approach to profile miRNAs in limited clinical samples. Am J Clin Exp Immunol. 2012; 1:70–89. [PubMed: 23304658]
27. Bronevetsky Y, et al. T cell activation induces proteasomal degradation of Argonaute and rapid remodeling of the microRNA repertoire. J Exp Med. 2013; 210:417–432. [PubMed: 23382546]
28. Hsu SD, et al. miRTarBase: a database curates experimentally validated microRNA-target interactions. Nucleic Acids Research. 2010; 39:D163–D169. [PubMed: 21071411]
29. Mavrakis KJ, et al. Genome-wide RNA-mediated interference screen identifies miR-19 targets in Notch-induced T-cell acute lymphoblastic leukaemia. Nat Cell Biol. 2010; 12:372–379. [PubMed: 20190740]
30. Gantier MP, et al. A miR-19 regulon that controls NF-B signaling. Nucleic Acids Research. 2012; 40:8048–8058. [PubMed: 22684508]
31. Mingueneau M, et al. The transcriptional landscape of αβ T cell differentiation. Nat Immunol. 2013; 14:619–632. [PubMed: 23644507]
32. Olive V, et al. A component of the mir-17-92 polycistronic oncomir promotes oncogene-dependent apoptosis. Elife. 2013; 2:e00822. [PubMed: 24137534]
33. Srivastava N, Sudan R, Kerr WG. Role of Inositol Poly-Phosphatases and Their Targets in T Cell Biology. Front Immunol. 2013; 4:288. [PubMed: 24069021]
34. Di Cristofano A, et al. Impaired Fas response and autoimmunity in Pten+/- mice. Science. 1999; 285:2122–2125. [PubMed: 10497129]
35. Palmer DC, Restifo NP. Suppressors of cytokine signaling (SOCS) in T cell differentiation, maturation, and function. Trends Immunol. 2009; 30:592–602. [PubMed: 19879803]

36. Tanaka K, et al. Loss of suppressor of cytokine signaling 1 in helper T cells leads to defective Th17 differentiation by enhancing antagonistic effects of IFN-gamma on STAT3 and Smads. J Immunol. 2008; 180:3746–3756. [PubMed: 18322180]
37. Egwuagu CE, et al. Suppressors of cytokine signaling proteins are differentially expressed in Th1 and Th2 cells: implications for Th cell lineage commitment and maintenance. J Immunol. 2002; 168:3181–3187. [PubMed: 11907070]
38. Fujimoto M, et al. A regulatory role for suppressor of cytokine signaling-1 in T(h) polarization in vivo. Int Immunol. 2002; 14:1343–1350. [PubMed: 12407025]
39. Dickensheets H, et al. Suppressor of cytokine signaling-1 is an IL-4-inducible gene in macrophages and feedback inhibits IL-4 signaling. Genes Immun. 2006; 8:21–27. [PubMed: 17093501]
40. Tamiya T, Kashiwagi I, Takahashi R, Yasukawa H, Yoshimura A. Suppressors of Cytokine Signaling (SOCS) Proteins and JAK/STAT Pathways: Regulation of T-Cell Inflammation by SOCS1 and SOCS3. Arteriosclerosis, Thrombosis, and Vascular Biology. 2011; 31:980–985.
41. Coornaert B, et al. T cell antigen receptor stimulation induces MALT1 paracaspase–mediated cleavage of the NF-κB inhibitor A20. Nat Immunol. 2008; 9:263–271. [PubMed: 18223652]
42. Liu F, Qin HB, Xu B, Zhou H, Zhao DY. Profiling of miRNAs in pediatric asthma: upregulation of miRNA-221 and miRNA-485-3p. Mol Med Rep. 2012; 6:1178–1182. [PubMed: 22895815]
43. Bhakta NR, Woodruff PG. Human asthma phenotypes: from the clinic, to cytokines, and back again. Immunol Rev. 2011; 242:220–232. [PubMed: 21682748]
44. Rodriguez A, et al. Requirement of bic/microRNA-155 for normal immune function. Science. 2007; 316:608–611. [PubMed: 17463290]
45. Thai TH, et al. Regulation of the germinal center response by microRNA-155. Science. 2007; 316:604–608. [PubMed: 17463289]
46. Malmhäll C, et al. MicroRNA-155 is essential for TH2-mediated allergen-induced eosinophilic inflammation in the lung. J Allergy Clin Immunol. 201310.1016/j.jaci.2013.11.008
47. Collison A, Mattes J, Plank M, Foster PS. Inhibition of house dust mite-induced allergic airways disease by antagonism of microRNA-145 is comparable to glucocorticoid treatment. J Allergy Clin Immunol. 2011; 128:160–167.e4. [PubMed: 21571357]
48. Kumar M, et al. Let-7 microRNA-mediated regulation of IL-13 and allergic airway inflammation. J Allergy Clin Immunol. 2011; 128:1077–85.e1–10. [PubMed: 21616524]
49. Sharma A, et al. Antagonism of mmu-mir-106a attenuates asthma features in allergic murine model. J Appl Physiol. 2012; 113:459–464. [PubMed: 22700801]
50. Edwards MR, et al. Targeting the NF-κB pathway in asthma and chronic obstructive pulmonary disease. Pharmacology and Therapeutics. 2009; 121:1–13. [PubMed: 18950657]
51. Suzuki A, et al. T cell-specific loss of Pten leads to defects in central and peripheral tolerance. Immunity. 2001; 14:523–534. [PubMed: 11371355]
52. Chen C, et al. Integrin α9β1 in airway smooth muscle suppresses exaggerated airway narrowing. J Clin Invest. 2012; 122:2916–2927. [PubMed: 22772469]

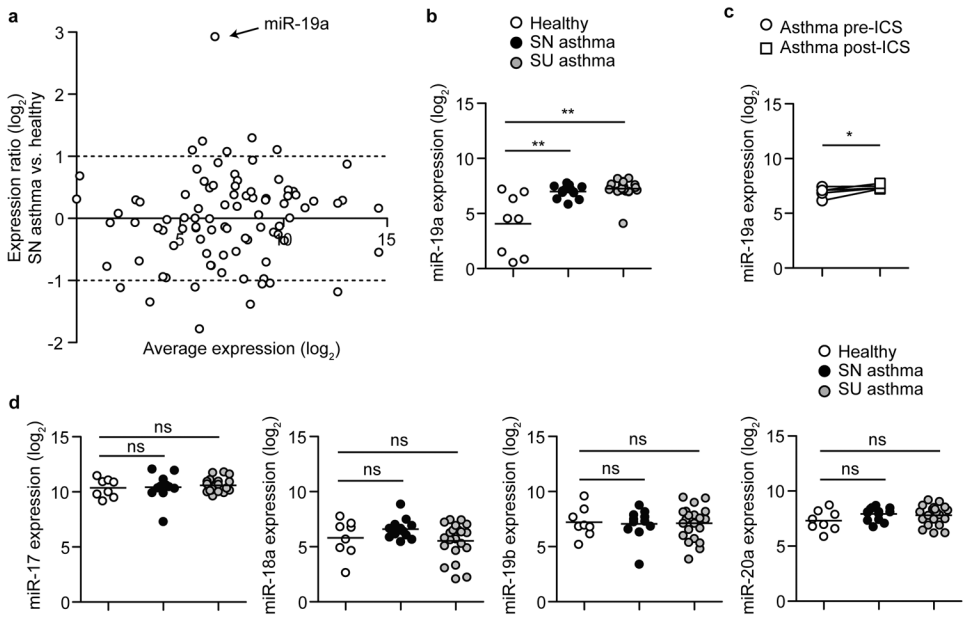

Figure 1. miR-19a expression is elevated in CD4$^+$ T cells from asthmatic lungs

(**a**) Taqmanq PCR analysis of miRNA expression in sorted CD4 T cells. Circles represent global-mean-normalized average miRNA expression in asthma compared to healthy subjects. Dashed lines represent 2-fold higher or lower expression. (**b**) qPCR analysis of miR-19a expression normalized to the global mean. Circles represent individual subjects. Line represents mean expression for each group. (**c**) qPCR analysis of miR-19a expression in CD4$^+$ T cells from individual asthmatic subjects pre- and post- 6 weeks of inhaled corticosteroid (ICS) treatment. $n = 5$. (**d**) qPCR analysis of the expression of miR-17, miR-18a, miR-19b, and miR-20a (members of the miR-17∼92 cluster; miR-92a was not detected in this experiment) normalized to the global mean. Circles represent individual subjects. Lines represent mean expression for each group.(**a-d**) Data are pooled from 2 experiments with $n = 8$ Healthy, 13 steroid-naïve (SN) asthma, and 21 steroid-using (SU) asthma. (**b, d**) One-way ANOVA with Dunnett's post test (compared to healthy). (**c**) Paired 2-tailed t-test. *p < 0.05, **$p < 0.0001$, ns = not significant.

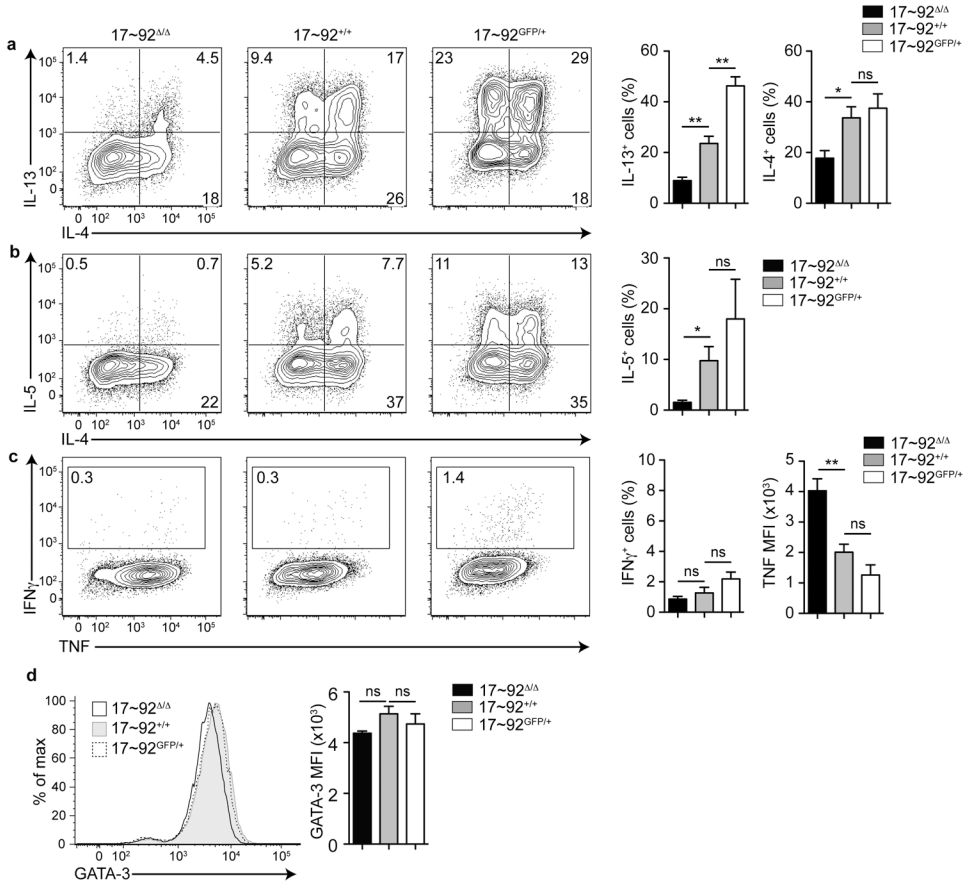

Figure 2. The miR-17∼92 cluster promotes T_H2 cytokine production

(**a-c**) Intracellular cytokine staining and pooled analysis of day 5 T_H2-polarized CD4$^+$ T cells from 17∼92$^{\Delta/\Delta}$ (left), 17∼92$^{+/+}$ (middle), and 17∼92$^{GFP/+}$ (right) mice. Numbers in quadrants indicate percentage of cells producing the indicated cytokine among live singlets. Bar graphs indicate total cytokine$^+$ cells as a percentage of live singlets. Error bars are mean ± SEM. (**a**) Flow cytometry data is representative of 11 independent experiments. *n*= 12 17∼92$^{\Delta/\Delta}$ (black), 17 17∼92$^{+/+}$ (grey), and 6 17∼92$^{GFP/+}$ (white) mice pooled from 11 independent experiments. (**b**) Flow cytometry data is representative of 7 independent experiments. *n* = 8 17∼92$^{\Delta/\Delta}$ (black), 10 17∼92$^{+/+}$ (grey), and 4 17∼92$^{GFP/+}$ (white) mice pooled from 7 independent experiments. (**c**) Flow cytometry data is representative of 11 independent experiments. *n* = 12 17∼92$^{\Delta/\Delta}$ (black), 17 17∼92$^{+/+}$ (grey), and 7 17∼92$^{GFP/+}$ (white) mice pooled from11 independent experiments. (**d**) Flow cytometry of GATA-3 expression in day 5 T_H2-polarized CD4 T cells from 17∼92$^{\Delta/\Delta}$ (black line), 17∼92$^{+/+}$ (grey filled), and 17∼92$^{GFP/+}$ (black dashed line) mice. Data are representative of 2 experiments. Bar graph indicates mean fluorescence intensity (MFI) of GATA-3 expression in live singlets of 17∼92$^{\Delta/\Delta}$ (black), 17∼92$^{+/+}$ (grey), and 17∼92$^{GFP/+}$ (white) mice. Error bars are mean ± SEM. *n* = 4, 4, 4 (2 mice in each group with duplicate cultures from 2 independent experiments). (**a, c, d**) One-way ANOVA with Dunnett'spost test. (**b**) One-way ANOVA Kruskal-Wallis test (for groups with unequal variance) and Dunn's post test. *p< 0.05, **p< 0.001, ns = not significant.

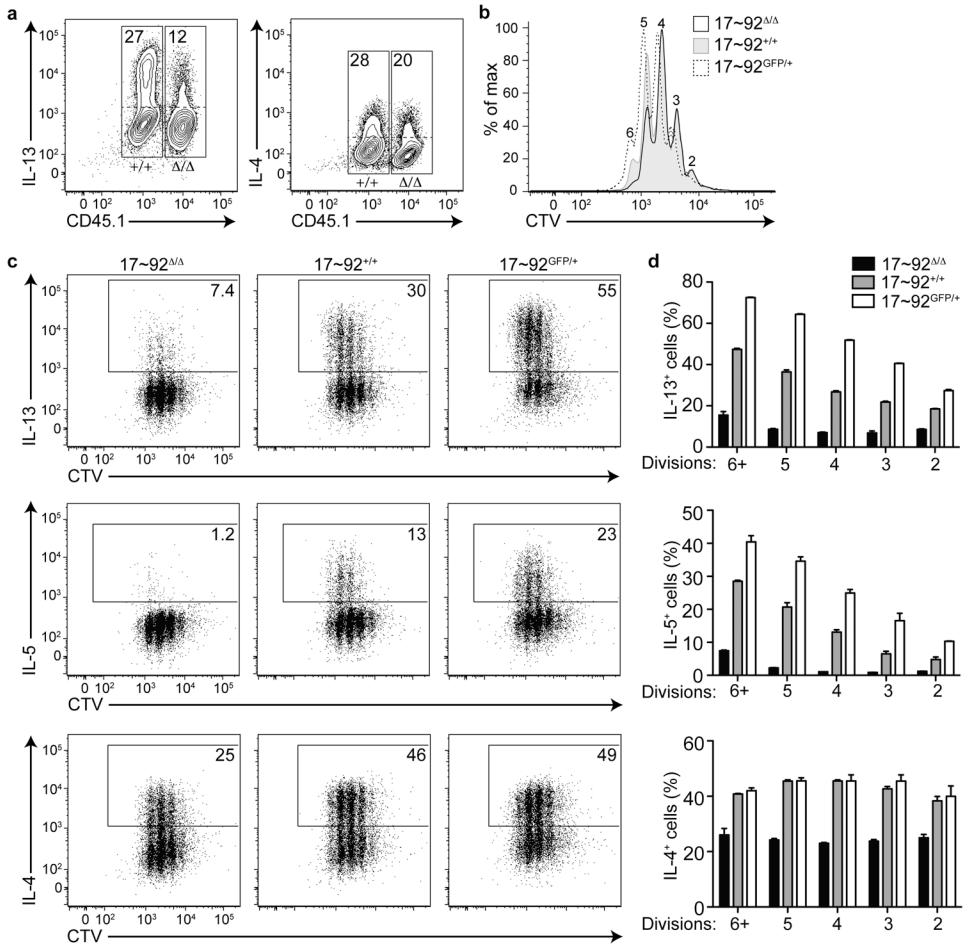

Figure 3. The miR-17∼92 cluster promotes T_H2 cytokine production in a cell-intrinsic and proliferation-independent manner

(**a**) Intracellular cytokine staining of $CD4^+$ T cells from $CD45.1^+$ $17{\sim}92^{\Delta/\Delta}$ and $CD45.2^+$ $17{\sim}92^{+/+}$ mice, co-cultured in T_H2 polarizing conditions for 5 days. Numbers indicate percentage of cytokine-producing cells (above the dotted line) in either the $CD45.1^+$ or the $CD45.1^-$ gate (solid boxes). Data are representative of 2 independent experiments with 2 mice each and duplicate cultures. (**b**) Cell Trace Violet (CTV) stain indicating proliferation of day 5 T_H2-polarized $17{\sim}92^{\Delta/\Delta}$ (black line), $17{\sim}92^{+/+}$ (grey filled), and $17{\sim}92^{GFP/+}$ (black dashed line) $CD4^+$ T cells. Numbers above peaks indicate division number relative to an undivided control. (**c**) Intracellular cytokine staining of CTV-labeled $17{\sim}92^{\Delta/\Delta}$ (left), $17{\sim}92^{+/+}$ (middle), and $17{\sim}92^{GFP/+}$ (right) day 5 T_H2-polarized $CD4^+$ T cells. Solid box indicates cytokine-positive gate used for quantification in (**d**). (**d**) Quantification of (**c**) showing cytokine-positive cells (as a percentage of live singlets) at each division in $17{\sim}92^{\Delta/\Delta}$ (black bars), $17{\sim}92^{+/+}$ (grey bars), and $17{\sim}92^{GFP/+}$ (white bars) cells. Data are from one representative experiment. Error bars are mean with range. $n = 2$ replicate cultures from one mouse of each genotype. $p < 0.0001$ by 2-way ANOVA comparing $17{\sim}92^{\Delta/\Delta}$ and $17{\sim}92^{+/+}$ in IL-13, IL-5, and IL-4. $p < 0.0001$ by 2-way ANOVA comparing $17{\sim}92^{+/+}$ and $17{\sim}92^{GFP/+}$ in IL-13 and IL-5. $p = 0.3153$ by 2-way ANOVA comparing $17{\sim}92^{+/+}$ and $17{\sim}92^{GFP/+}$ in IL-4. (**b-d**) Data are representative of 6 independent experiments with

$17{\sim}92^{\Delta/\Delta}$ and $17{\sim}92^{+/+}$ (n = 6 mice each), and 2 experiments with $17{\sim}92^{+/+}$ and $17{\sim}92^{GFP/+}$ (n = 2 mice each).

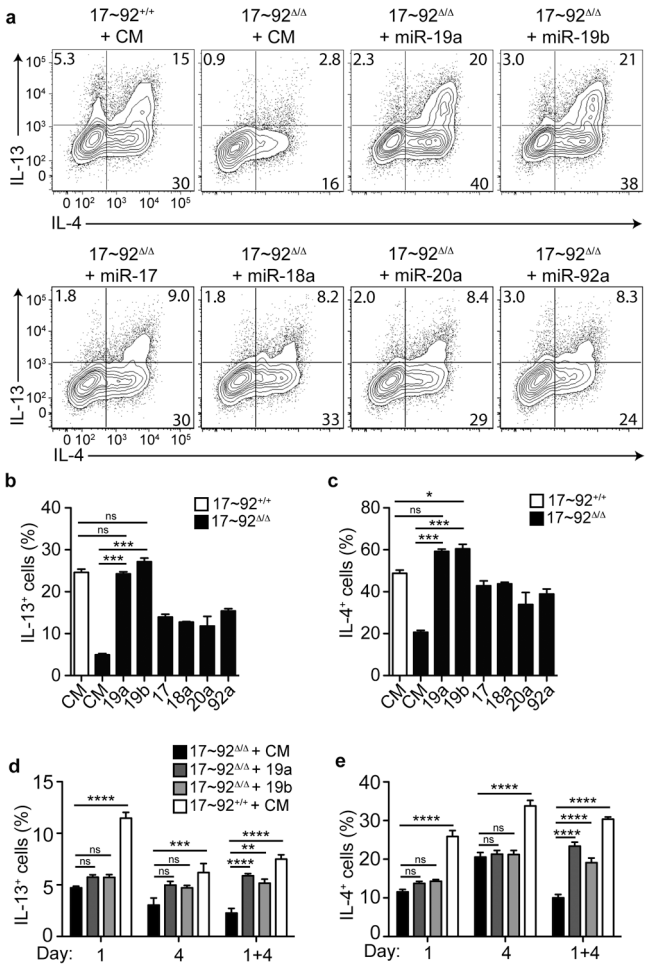

Figure 4. miR-19a and miR-19b rescue the T_H2 cytokine defect in 17∼92$^{Δ/Δ}$ cells

(**a**) Intracellular cytokine staining of 17∼92$^{+/+}$ or 17∼92$^{Δ/Δ}$ CD4 T cells transfected with control mimic (CM), miR-19a, -19b, -17, -18a, -20a, or -92a mimics. Cells were transfected on days 1 and 4 of T_H2 polarization, and analyzed on day 5. Numbers in each quadrant indicate percentage of cells producing the indicated cytokine. Data are representative of 3 independent experiments. (**b-c**) Quantification of IL-13 (**b**) or IL-4 (**c**) production at day 5 after transfection with miRNA mimics. Bars represent mean ± SEM for 3 individual transfections for each condition. Data are representative of 3 independent experiments. (**d-e**) 17∼92$^{+/+}$ or 17∼92$^{Δ/Δ}$ CD4$^+$ T cells were transfected with CM, miR-19a, or -19b on day 1 only, day 4 only, or both day 1 and 4. Quantification of IL-13 (**d**) or IL-4 (**e**) production at day 5 of T_H2 polarization. Error bars are mean ± SEM for 3 individual transfections for each condition. Data are representative of 2 independent experiments. (**b, c**) One-way ANOVA with Dunnett's post test (comparing each column to 17∼92$^{Δ/Δ}$ + CM). (**d, e**) $p < 0.0001$ by 2-way ANOVA with Bonferroni post test (comparing each column to 17∼92$^{Δ/Δ}$ + CM per time point). ns = "not significant", *$p < 0.05$, ** $p < 0.01$, *** $p < 0.001$, ****$p < 0.0001$.

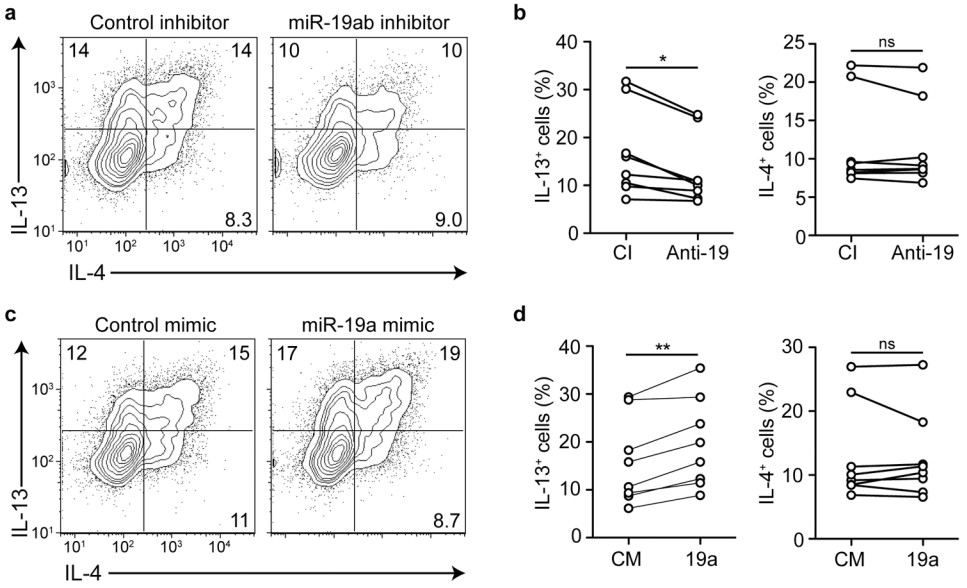

Figure 5. miR-19a promotes IL-13 production in human CD4$^+$ T cells

(**a**) Intracellular cytokine staining of CD4$^+$ T cells isolated from human cord blood and transfected with control inhibitor or anti-miR-19 inhibitor on days 1 and 4 in T_H2 polarizing conditions, analyzed on day 5. Numbers in each quadrant indicate percentage of cytokine-positive cells. Data are representative of 3 experiments with 8 cord blood samples. (**b**) Quantification of IL-13 (left) or IL-4 (right) producing human CD4$^+$ T cells upon transfection with control inhibitor (CI) or anti-miR-19 inhibitor (Anti-19). Circles represent the mean of 2 individual transfections of each inhibitor. Lines connect individual cord blood donors receiving either inhibitor. n = 8 cord bloods in 3 experiments. (**c**) Intracellular cytokine staining of CD4$^+$ T cells isolated from human cord blood and transfected with control mimic or miR-19a mimic on days 1 and 4 in T_H2 polarizing conditions, analyzed on day 5. Numbers in each quadrant indicate percentage of cytokine-positive cells. Data are representative of 3 experiments with 8 cord blood samples. (**d**) Quantification of IL-13 (left) or IL-4 (right) producing human CD4$^+$ T cells upon transfection with control mimic (CM) or miR-19a mimic (19a). Circles represent the mean of 2 individual transfections of each mimic. Lines connect individual cord blood donors receiving either mimic. n = 8 cord bloods in 3 experiments. (**b, d**) Two-tailed paired t-test. *$p < 0.01$, **$p < 0.001$, ns = not significant.

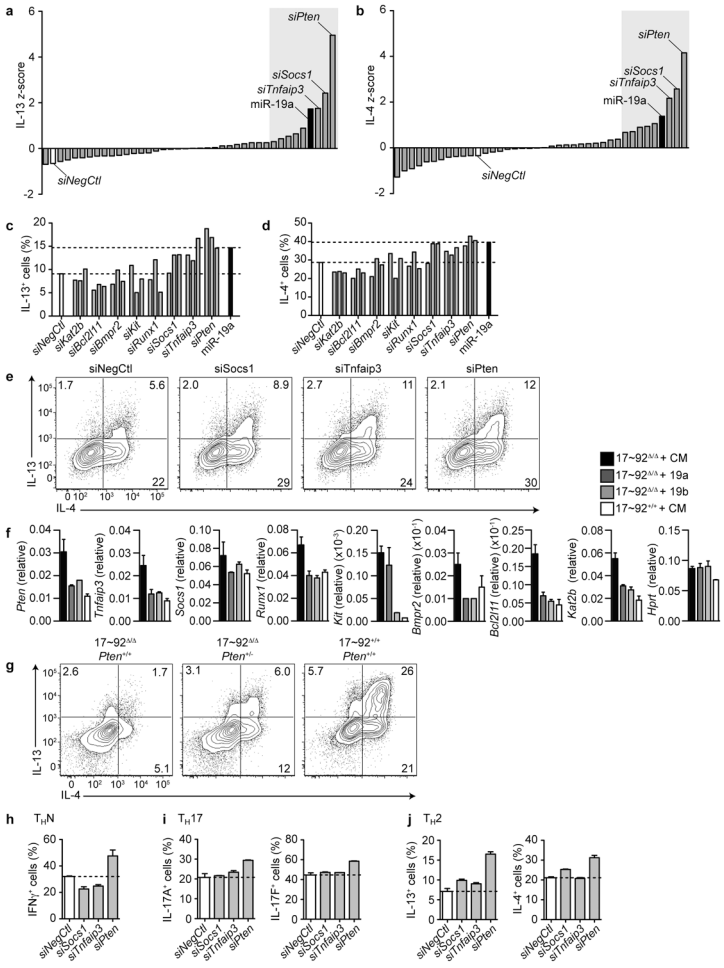

Figure 6. Several miR-19 targets negatively regulate T_H2 cytokine production

(**a-b**) Primary screen of miR-19 targets that alter IL-13 and IL-4 production. Analysis of intracellular cytokine staining of 17∼92$^{\Delta/\Delta}$ cells transfected with 38 siRNA smart pools. Bars indicate IL-13 *z*-score (z = x – mean/SD where x represents the IL-13$^+$ cells (%) for each siRNA (**a**) or IL-4 *z*-score (**b**). The white bar indicates siRNA nontargeting control (siNegCtl), and the black bar indicates miR-19a mimic positive control. The shaded grey area highlights the 8 genes with further analysis in (**c**) and (**d**). Data are representative of two independent experiments. (**c-d**) Analysis of intracellular cytokine staining of 17∼92$^{\Delta/\Delta}$ cells transfected with 3 individual siRNAs against the top 8 candidate genes identified in (**a**) and (**b**). Bars indicate IL-13$^+$ (**c**) and IL-4$^+$ (**d**) cells as a percentage of live singlets. The white bar indicates siNegCtl, and the black bar indicates miR-19a mimic. Dashed lines indicate the range between the negative and positive controls. Data are representative of 2 independent experiments. (**e**) Intracellular cytokine staining of 17∼92$^{\Delta/\Delta}$ cells transfected with individual siRNAs against *Socs1, Tnfaip3,* and *Pten* compared to siNegCtl. Numbers in each quadrant indicate percent of cytokine-positive cells. Data are representative of 4 independent experiments. (**f**) qPCR expression of the top 8 candidate miR-19a targets in 17∼92$^{\Delta/\Delta}$ cells transfected with control (CM, black bars), miR-19a (dark grey bars), miR-19b (light grey bars) mimics, or 17∼92$^{+/+}$ cells transfected with CM (white bars). Data

are normalized to *Gapdh*. Data are representative of 2 independent experiments. Error bars represent mean with range of 2 technical replicates. (**g**) Intracellular cytokine stain of day 5 "Low T_H2"-polarized cells from $17{\sim}92^{\Delta/\Delta}$ $Pten^{+/+}$ (left), $17{\sim}92^{\Delta/\Delta}$ $Pten^{+/-}$ (middle), and $17{\sim}92^{+/+}$ $Pten^{+/+}$ mice. Numbers in each quadrant indicate percent of cytokine-positive cells. Data are representative of two experiments. (**h-j**) Analysis of intracellular cytokine staining of $17{\sim}92^{\Delta/\Delta}$ cells in non-polarizing (**h**), T_H17 polarizing (**i**), or T_H2 polarizing (**j**) conditions transfected with individual siRNAs against *Socs1*, *Tnfaip3*, and *Pten*, compared to siNegCtl. Bars represent mean with range. $n = 2$ transfections for each condition. Data are representative of 2 independent experiments.

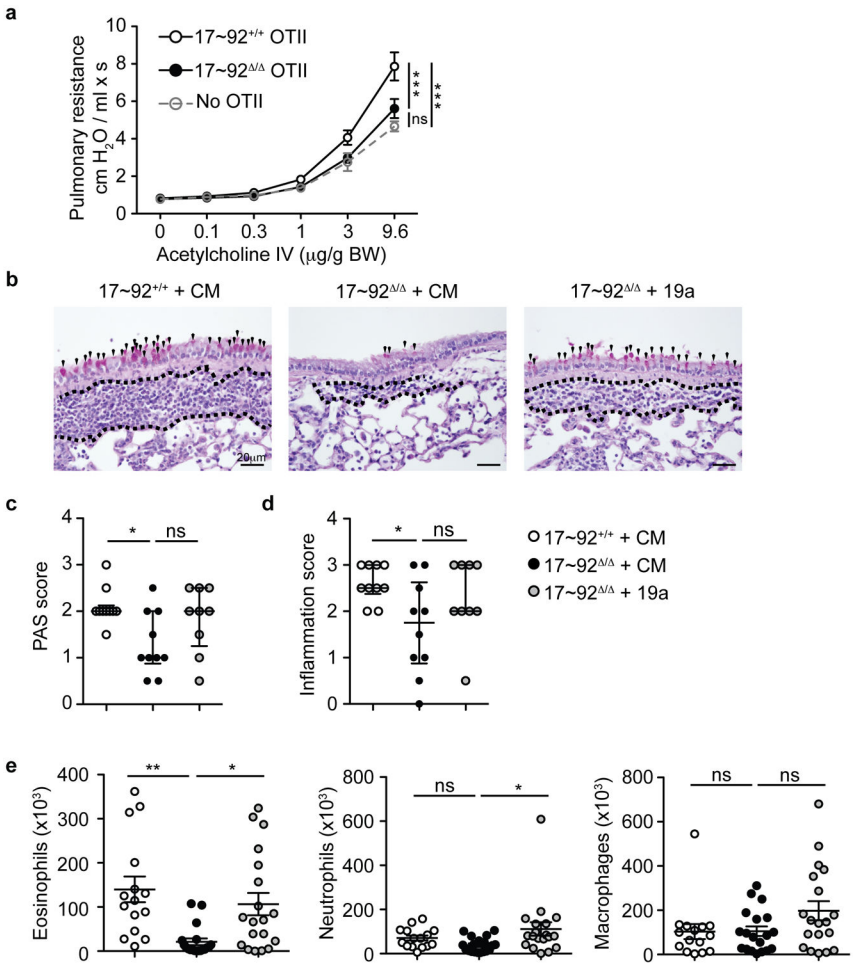

Figure 7. The miR-17∼92 cluster promotes T_H2-driven inflammation *in vivo*

(**a**) Pulmonary resistance measures at day 4 in response to increasing doses of acetylcholine. Circles represent mean of 10 mice receiving 17∼92$^{+/+}$ OT-II cells (black line open circles), 10 mice receiving 17∼92$^{\Delta/\Delta}$ OT-II cells (black line black circles), and 6 mice receiving no cells (grey dashed line open circles). Error bars represent mean ± SEM. Statistics on the plot indicate differences at the highest dose of acetylcholine. Data from 2 experiments were combined. (**b**) Representative Periodic Acid Schiff (PAS) staining of lung sections from recipient mice with 17∼92$^{+/+}$ OT-II cells transfected with control mimic (CM) (left; *n* = 10), 17∼92$^{\Delta/\Delta}$ OT-II cells transfected with CM (middle; *n* = 10), or 17∼92$^{\Delta/\Delta}$ OT-II transfected with miR-19a mimic (right; *n* = 9). Images are representative of 2 experiments. Black arrowheads mark PAS^{+} cells. The area between the dotted lines indicates immune cell infiltration. (**c-d**) Histologic scores of PAS staining (**c**) to quantify mucus-secreting cells, and H&E staining (**d**) to quantify airway inflammation. Error bars represent median with inter quartile range. Analyses use a scale 0-4 and are analyzed by a blinded observer.(**e**) Analysis of flow cytometry of inflammatory cells in the BAL on day 4. Eosinophils (CD11b^{+} Siglec F^{+}, left), neutrophils (CD11b^{+} Ly6G^{+}, middle), and alveolar macrophages (CD11c^{+} Siglec F^{+}, right) were quantified as the product of their frequency among live cells and the total BAL cell count. Error bars represent mean ± SEM. *n* = 15, 19, and 19. (**a**) Two-

way ANOVA with Bonferroni post-tests. (**c-e**) One-way ANOVA with Dunnett's post test. *$p < 0.05$, **$p < 0.001$, ***$p < 0.0001$. ns = not significant.

Table 1

Healthy and asthmatic subjects providing bronchoalveolar lavage CD4 T cells for miRNA expression analysis

	Healthy	Steroid-naïve Asthma	Steroid-using Asthma
Sample size (M/F)	8 (4/4)	14 (5/9)	21 (9/12)
Age, y	40.3 (25-56)	30.1 (20-56)	37.3 (18-55)
FEV1 % predicted	100 (88-128)	90 (61-103)	80 (59-110)
Methacholine PC_{20} mg/ml	>10	0.8 (0.08-4.3)	2.1 (0.14-8.1)
Sorted $CD4^+$ T cells ($\times 10^3$)	215 (24-440)	243 (29-1,250)	277 (45-2,200)